Biochemical and Biophysical Research Communications 376 (2008) 40–45

Contents lists available at ScienceDirect

Biochemical and Biophysical Research Communications

journal homepage: www.elsevier.com/locate/ybbrc

Novel mitochondrial extensions provide evidence for a link between microtubule-directed movement and mitochondrial fission

Timothy Bowes, Radhey S. Gupta *

Department of Biochemistry and Biomedical Sciences, McMaster University, Hamilton, Canada L8N 3Z5

ARTICLE INFO

Article history:
Received 14 August 2008
Available online 31 August 2008

Keywords:
Ethacrynic acid
N-Ethylmaleimide
Mitochondrial fusion and fission dynamics
Mitochondrial extensions
Drp-1
Microtubule motors

ABSTRACT

Mitochondrial dynamics play an important role in a large number of cellular processes. Previously, we reported that treatment of mammalian cells with the cysteine-alkylators, *N*-ethylmaleimide and ethacrynic acid, induced rapid mitochondrial fusion forming a large reticulum approximately 30 min after treatment. Here, we further investigated this phenomenon using a number of techniques including live-cell confocal microscopy. In live cells, drug-induced fusion coincided with a cessation of fast mitochondrial movement which was dependent on microtubules. During this loss of movement, thin mitochondrial tubules extending from mitochondria were also observed, which we refer to as 'mitochondrial extensions'. The formation of these mitochondrial extensions, which were not observed in untreated cells, depended on microtubules and was abolished by pretreatment with nocodazole. In this study, we provide evidence that these extensions result from of a block in mitochondrial fission combined with continued application of motile force by microtubule-dependent motor complexes. Our observations strongly suggest the existence of a link between microtubule-based mitochondrial trafficking and mitochondrial fission.

Mitochondria are dynamic organelles able to undergo dramatic morphological changes which depend on the balance of mitochondrial fusion and fission rates, as well as directed movement and/or anchoring along the various components of the cytoskeleton, such as microfilaments, microtubules (MTs) and intermediate filaments [1–5]. Mitochondrial morphology also varies greatly ranging from highly fragmented punctate vesicles during apoptosis, to large fused reticuli seen in *Drosophila* sperm axoneme and in mating yeast [1,2,6–8]. Although the specific purpose(s) of such morphological changes remains unclear, alterations in mitochondrial morphology have been linked to Ca^{2+} signaling and buffering, apoptosis, the cell cycle, embryonic development, and neuronal disease [9–13].

Work during the past decade has led to identification of several essential protein components of the mitochondrial fusion and fission machinery including dynamin-related protein 1 (Drp1), Fis1, Opa1, and the mitofusions [1,2,12,14–16]. Currently, the only tools available to study mitochondrial dynamics are siRNA (or RNAi) or dominant-negative mutants affecting the expression of these proteins [14,15]. However, the effects of these interventions can only be observed on a time scale of hours to days. In contrast, changes in mitochondrial morphology occur on a times-scale of minutes (e.g. vesicularization and fission after exposure to antimycin) [17] to seconds (e.g. completion of an individual mitochondrial fission event) [5]. We previously described a novel effect of the cysteine-alkylators, ethacrynic acid (EA) and *N*-ethylmaleimide (NEM), on mitochondrial dynamics [18,19]. These compounds begin to induce mitochondrial fusion and reticulum formation approximately 15–20 min after drug exposure [18,19]. No other compounds to date have shown similar effects on mitochondria. However, their target and mechanism with regards to the fusion/fission dynamic remains unknown. Thus, in this work, live-cell confocal microscopy is used to investigate how these compounds act on mitochondria. The results also provide novel insight concerning a link between the microtubule-based motility and mitochondrial fission.

Materials and methods

Cell culture and inhibitors. Using B-SC-1 African green monkey kidney cells, a cell line stably expressing mitochondrial matrix-targeted enhanced green fluorescent protein (eGFP) was selected by transfecting with the plasmid vector pMTS-eGFP, in which the MTS from cytochrome *c* oxidase subunit VIII has been fused to the N-terminal end of eGFP gene [20]. Cells were then grown in media containing 600 μg/mL neomycin analog G418 and selected for resistance. The resulting colonies were examined by fluorescence microscopy for expression of eGFP in the mitochondrial matrix compartment. The sources of various drugs viz. ECA,

* Corresponding author. Fax: +1 905 522 9033.
E-mail address: bowestj@mcmaster.ca (R.S. Gupta).

0006-291X/$ - see front matter © 2008 Elsevier Inc. All rights reserved.
doi:10.1016/j.bbrc.2008.08.120

NEM, nocodazole, and their stock concentrations are described in earlier work [18,19]. All drugs were diluted into α-MEM media immediately prior to use to give the desired final concentration. Where used as a drug stock solvent, ethanol concentration was kept to <1%, at which there were no gross observable effects on cell growth (based on cloning efficiency assay) or mitochondrial morphology (based on electron microscopy ultrastructure).

Live-cell imaging and electron microscopy. B-SC-1 cells stably expressing mito-eGFP were grown on 0.17 mm Delta T heated dishes (Bioptechs, Butler, PA, USA) in 5% fetal calf serum supplemented α-MEM at 37 °C. Live cells were observed using a Yokogawa spinning disk confocal unit, an LMM5 spectral laser merge module, and an ultrafast Hamamatsu back-thinned EMCCD C9100-12 camera equipped with a whole-microscope LiveCell2 temperature and CO_2 environment control system (Quorum) (McMaster Biophotonics Facility, McMaster University, Hamilton, ON, Canada). Confocal images were taken every 10 s and laser power was adjusted to minimize phototoxicity and retain image quality. NIH ImageJ software was used to analyze the resulting images. Analysis of mitochondrial fast movement and extension events was accomplished using the Point Picker plugin (Philippe Thévenaz, Biomedical Imaging Group, Swiss Federal Institute of Technology, Lausanne, Switzerland). Manual particle tracking was performed using the Manual Tracking plugin for NIH ImageJ.

For electron microscopy, B-SC-1 cells were also fixed in 2% glutaraldehyde in 0.1 M sodium cacodylate buffer (pH 7.4) for 1 h at 4 °C. Cells were post-fixed with 1% OsO_4 and then serially dehydrated in ethanol. The processing of post-fixed cells in Spurr's resin and their imaging is described in our earlier work [21].

Results

Characterization of mitochondrial extensions after drug-induced mitochondrial fusion

Previously, we showed that EA or NEM induced mitochondrial fusion in cultured mammalian cells at sub-toxic concentrations [18,19]. Using eGFP expressing B-SC-1 cells combined with a spinning disk confocal microscope, we were able to obtain high quality images with minimal phototoxicity and photobleaching.

Live B-SC-1 cells were imaged for 30 min before the addition of drug (viz. 30 μM NEM) and for up to 60 min afterwards (see supplementary movie 1). Fig. 1A and B show the overall fusogenic effect of 30 μM NEM after 60 min. Before NEM, mitochondria displayed changes in movement and morphology observed by others [22,23]. This included fast, directed saltatory movement, away from, or towards the nucleus, indicative of MT-based movement, as well as slow, undirected movement. Both fission and fusion actively occurred, sometimes consecutively, involving the same mitochondria. In Fig. 1C, a mitochondrion underwent two separate fission events (before addition of 30 μM NEM) while displaying fast MT-directed movement in an anterograde manner. Only one of the two 'daughter' mitochondria from each fission event continued this movement, presumably still being pulled along the MT, while the other two became immotile.

Approximately 25 min after addition of 30 μM NEM, fast mitochondrial movement was no longer observed and thin mitochondrial extensions formed from mitochondria. These extensions coincided temporally with the onset of mitochondrial fusion. Fig. 1D shows the formation of three separate extensions during the given time frame. Out of these three, one forms and immediately retracts into its originating mitochondrion in the fourth frame.

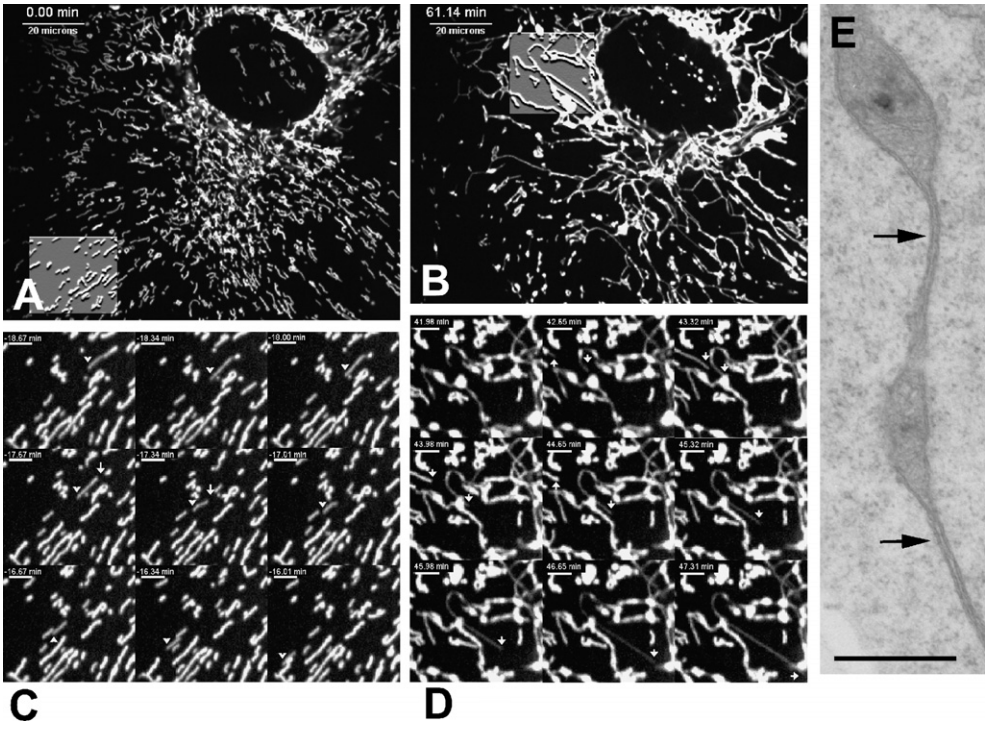

Fig. 1. (A–D) Time-course showing a series of confocal images of a live mito-eGFP B-SC-1 cell before and after treatment with 30 μM NEM. (A,C) before NEM treatment; (B,D) after NEM treatment. The time after addition of NEM is indicated in the upper left of each frame. NEM was added at 0 min. The highlighted regions in (A,B) are shown in (C,D). (C) A fast moving mitochondrion (white arrowheads). Two fission events (white arrows) begin in frames 3 and 4, and both result in immotile daughter mitochondrion. (D) The formation of two mitochondrial extensions (white arrowheads). Both extensions begin forming in frame 2. The first retracts into its originating mitochondrion in frame 6, while the other extending through to frame 9. (A,B) Scale bars indicate 20 μm. C and D: Scale bars indicate 5 μm. (E) An electron micrograph from B-SC-1 cells treated for 1 h with 30 μM NEM. The arrows indicate very thin mitochondrial tubules which likely represent elongated extensions which later became fused. Scale bar indicates 500 nm.

Another extension forms and retracts in the fourth and fifth frame while a third extension elongates until the ninth frame then fuses to another section of the forming reticulum. This data typified mitochondrial extension behavior, in that they sometimes fused to other mitochondria and became fixed in an extended tubule conformation and or else retracted into their originating mitochondrion. Additionally, extension length varied greatly, from less than 1 μm (i.e. based on an approximate 0.25 μm per pixel resolution) to greater than 30 μm. Similar results were obtained in experiments where cells were treated with 60 μg/mL of EA (data not shown). We also used a transmission electron microscope to examine the ultrastructure of mitochondrial extensions in B-SC-1 cells treated with 30 μM NEM. Fig. 1E shows an image of an approximately 50 nm wide mitochondrial tubule connecting two larger mitochondria which may represent an extension which fused just prior to fixation.

Mitochondria undergoing fast MT-based movement have long been known to display a typical saltatory movement [5,22,24]. This type of movement was qualitatively observed in both fast movements and extension formation (see supplementary movie 1). To test whether extensions were related to fast MT-based movement, their velocities were quantified and compared. As mentioned previously, however, mitochondria also undergo a slow directionless Brownian-like motion. Thus, a cutoff value of the average measured velocity of the Brownian-like motion (0.1 ± 0.1 μm/0 s interval over all experiments) was used to remove velocities deemed too low for each experiment. The results of these measurements revealed that the velocities of the mitochondrial extensions were significantly different but on the same order as that of fast mitochondrial movement, that is, approximately 2.6 ± 0.2 μm/10 s interval ($N = 3$, $n = 10$) versus 3.8 ± 0.1 μm/10 s per interval ($N = 3$, $n = 20$) for the fast mitochondrial movement. These results showed that extensions were qualitatively similar, but on average slightly slower than fast MT-based movement.

Mitochondrial extensions require microtubules

To determine whether mitochondrial extensions were dependent upon MTs, the effect of nocodazole (Nz), a MT-disrupting agent, in live cells was examined. Fig. 2 shows the results of this experiment. Cells were treated with 10 μM Nz for 2 h prior to the beginning of the experiment. After 30 min of image acquisition, 30 μM NEM was added and imaging continued for another 60 min. In control cells not treated with Nz, mitochondrial extensions still formed. However, in cells that pretreated with Nz (disruption of MTs was confirmed by immunofluorescent labeling with tubulin antibody; data not shown), mitochondrial length and thickness increased and they became disoriented and spread out within the cytosol (Fig. 2; right panel). Mitochondria in these cells still displayed a type of fast movement, which is best described as neither retrograde or anterograde, overall. This may be due to trafficking along other known cytoskeletal systems, such as actin microfilaments, as has been observed by others [23,24]. Interestingly, after NEM treatment, mitochondrial fusion was still able to occur, as also seen in earlier work [19]. However, no extension formation was observed (Fig. 2; left panel). In this case, mitochondrial fusion also only occurred between mitochondria which were already in close proximity to one another. This experiment suggests that the formation of mitochondrial extensions require the presence of intact MTs. It also suggests that extensions themselves are not required for mitochondrial fusion, even though they sometimes culminate in fusion events (Fig. 1D).

Mitochondrial extensions are temporally related to MT-based mitochondrial movement

Although, the above experiments suggested that extensions required MTs and that they also displayed velocities close to that

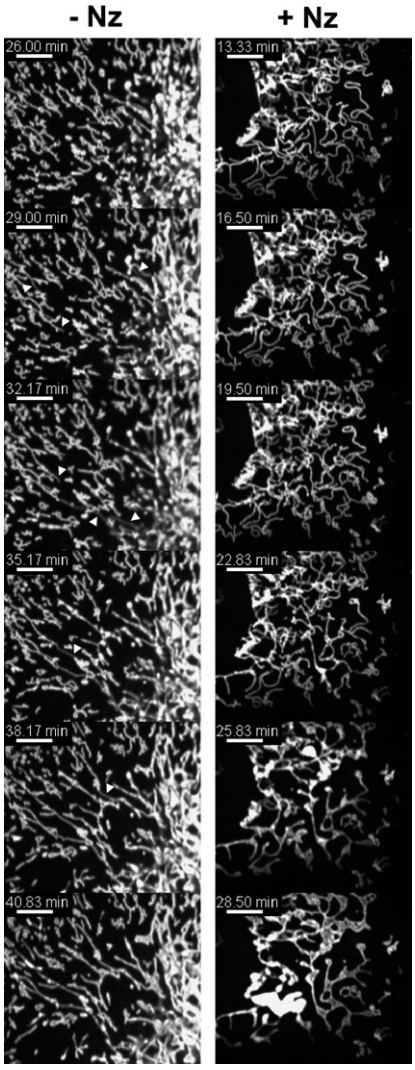

Fig. 2. Time-course showing confocal imaging of a live mito-eGFP B-SC-1 cell after treatment with 30 μM NEM with (+Nz) or without (−Nz) a 2 h pre-treatment with 10 μM nocodazole. Mitochondrial extensions are visible in the −Nz cell (first frame, column 1) (white arrowheads). Three extensions begin forming in the second frame, and a fourth and fifth extension begin forming in the third and fifth frames, respectively. Column 2 shows induced fusion in the +Nz cell, but no extensions formed. The time after addition of NEM is indicated. Scale bars indicate 10 μm.

of fast MT-based movement, it was still not clear whether the two processes were causally related. To understand if these events were related temporally, individual events were counted over the course of live-cell imaging experiments where one image was taken every 10 s. Live mito-eGFP cells were imaged by spinning disk confocal for 30 min before being treated with either 5 μM or 30 μM NEM for 90 min. The 5-μM treatment was used as a below-fusion threshold negative control. Due to the complex nature of fast mitochondrial movement and mitochondrial extension events, it was not possible to automate event counting using the ImageJ software, and instead, manual event counting was carried out. However, the Point Picker ImageJ plugin was used to eliminate the possibility of counting an event more than once. In cases of fast movement or extension formation where there was an abrupt directional change, only a single event was counted. Fig. 3 shows a histogram comparing these events over time. After 5 μM NEM, no major changes occurred in the distribution of fast movement events and the number of mitochondrial extensions observed

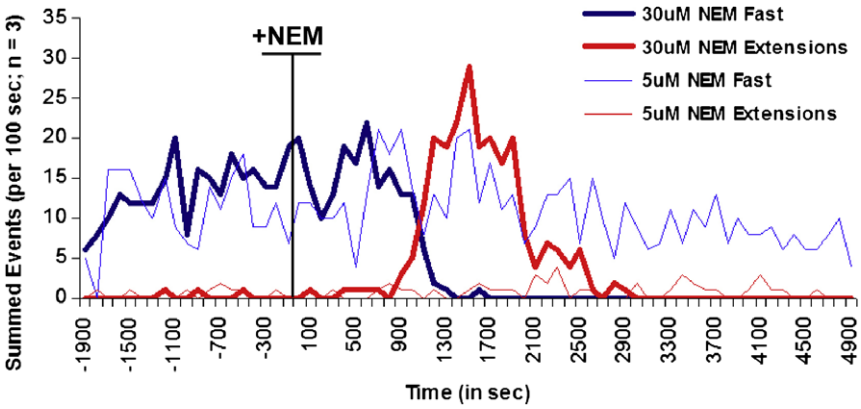

Fig. 3. A histogram of the summed counts of fast mitochondrial movement and mitochondrial extension formation events. The time frame used was from 30 min before and 90 min after treatment of either 5 μM or 30 μM NEM in mito-eGFP B-SC-1 cells. The vertical line indicates the time after addition of NEM. Bin size is 100 s (or 10 successive frames). $n = 3$ for each concentration of NEM used.

was extremely low and were quite short (i.e. less than 1 μm). In contrast, after 30 μM NEM, a sharp decrease in fast mitochondrial movement was observed between approximately 10 min ($t = 600$ s) and 25 min ($t = 1500$ s) (Fig. 3). Importantly, this decrease in fast movement was accompanied by a large increase in mitochondrial extensions.

Discussion

The goal of these studies was to further characterize the fusogenic effect of NEM and EA on mitochondrial dynamics. In this work, we report an additional effect of these drugs, that is, the formation of 'mitochondrial extensions' which occurred during same time frame as the loss of fast movement and the onset of mitochondrial fusion (Fig. 3 and supplementary movie 1). These extensions formed at a speed slightly slower than fast mitochondrial movement but their temporal appearance coincided with the almost complete cessation of MT-based fast mitochondrial movement. Further, the formation of these extensions (but not mitochondrial fusion itself) was abolished after MT-disruption by Nz pretreatment, providing strong evidence that while MTs are required for the formation of extensions, they are not necessary for the mitochondrial fusion (Fig. 2).

A simple encompassing explanation for these qualitative and quantitative observations is that mitochondrial extensions are the direct result of the continuation of normal MT-based fast mitochondrial movement during the inhibition of mitochondrial fission. In this way, the cessation of MT-based mitochondrial movement seen in Fig. 3 is merely the result of MT-based mitochondrial movement occurring under the guise of extension formation. The following (see Fig. 4) summarizes this explanation in light of the current understanding of mitochondrial fission in the literature and Fig. 1 is referred to for illustrative purposes. Before NEM treatment, each of the two fission events shown (see Fig. 1C) results in the immobilization of one daughter mitochondrion while the other continues moving. This is shown diagrammatically (steps 1–5), where a mitochondrion is pulled by a MT-based motor protein complex which is then followed by a mitochondrial fission event (steps 4 and 5). The steps 2* to 3* illustrate the result of the same type of event after NEM treatment. In this case, when a MT-motor attaches to an immobilized mitochondria that cannot undergo fission, the continuous action of the motor on the mitochondrion is proposed to lead to its elongation resulting in the formation of thin

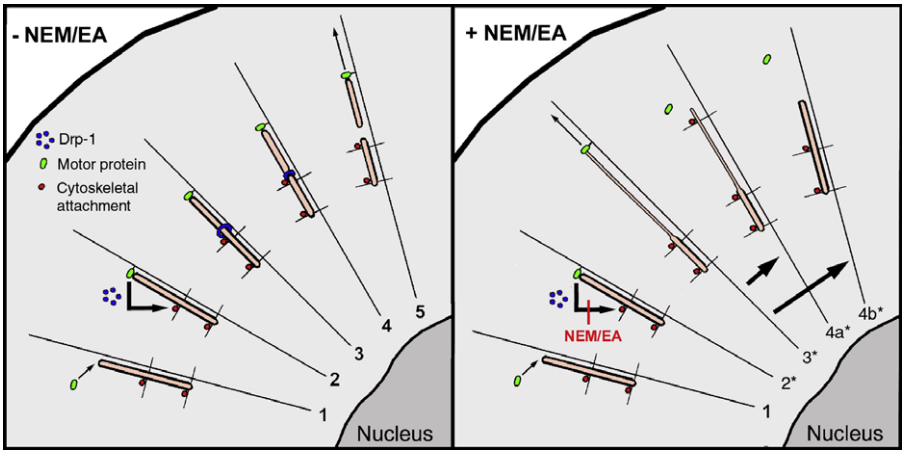

Fig. 4. A schematic diagram of the relationship between fast MT-based mitochondrial movement and extension formation. (Left panel, −NEM/EA): 1, MT motor complex (shown in green) binds an immobilized mitochondrion; 2, unknown signal(s) recruits fission complex components to a site prior to the closest mitochondrial–cytoskeletal attachment point (indicated by red text); 3, Drp1 fission complex (indicated by blue text) forms; 4, fission complex causes a mitochondrial fission event; 5, the motor complex can now pull the detached daughter mitochondrion along the MT. (Right panel, +NEM/EA): Step 1, the same as previous; 2*, NEM/EA interferes with recruitment or action of the fission complex at the closest mitochondrial-cytoskeletal attachment point; 3*, the motor complex continues to pull the immobilized mitochondria and forming an extension; 4a*, the extension binds to the cytoskeleton or fuses to another immobilized mitochondrion, stabilizing the newly formed extension and the motor complex is released, 4b*, the motor complex releases the mitochondrial extension and the mitochondrial extension retracts into the originating mitochondrion.

mitochondrial extensions that are observed in this work (see Fig. 1D).

According to this hypothesis, the large variability in extension length observed is likely at least partially dictated by the amount of total mitochondrial membrane available. A mitochondrion having only a small amount of extra membrane or 'slack' would only allow for the formation of a relatively short extension and vice versa. Our observation that some extensions (see Fig. 1D, upper left quadrant, frames 4–6) rapidly reverse back into their originating mitochondrion also fit well with this explanation. For example, it is possible that during extension formation, no additional attachment of the mitochondrial extension to the cytoskeleton or another mitochondrion takes place. In such an event, once released from the MT-based motor complex, the mitochondrial extension may snap back into its originating mitochondrion (see Fig. 4, steps 3* and 4b*). On the other hand, the attachment of mitochondrial extension to a cytoskeletal component or fusion to another mitochondrion might lead to stabilization of the extension (see Fig. 4, steps 3* and 4a*). Examples of can be seen in Fig. 1D and supplementary move 1. Also, the slower average speed of extension formation compared to fast MT-based movement (2.6 μm/10 s vs. 3.8 μm/10 s) also makes sense, in that, unlike free mitochondria, immobilized mitochondria likely exert a counter force on the MT-based motors.

Recently, Anesti et al. hypothesized that a type of "chemo attractant" might exist which specifically recruits the fission machinery to an immobilized mitochondrion in the event of its transport by a kinesin or dynein motor protein complex [4]. However, against this explanation other counter hypotheses could easily be made. For example, it could be stated that MT-based motor protein complexes are merely not recruited to immobilized mitochondria at all. It could also be argued that MT-based motor protein complexes are simply not able to apply enough force to pull an immobilized mitochondrion. Strikingly, however, the extensions characterized in this work counter these hypotheses and provide the first evidence that there is indeed a link between these two crucial systems. That is, the very existence of these mitochondrial extensions suggests that MT-based motors can still attach to and pull mitochondrial cargo which lacks the capacity for mitochondrial fission. Furthermore, based on this evidence it can be argued that if the attachment of the motor protein complex and mitochondrial fission were not intrinsically linked in some way, then mitochondrial extensions would be routinely observed in cells. Interestingly, observed overall elongation after disruption of MTs by Nz (see Fig. 2) also fits this hypothesis, as a lack of MT-based movement would result in a loss of related fission events, upsetting the fusion/fission dynamic leading to mitochondrial elongation.

Since the mechanisms of mitochondrial dynamics are still not well understood, the target responsible for this fission block remains difficult to predict. However, NEM sensitive factor (NSF) is a key regulator of membrane fusion in ER-Golgi transport, and was initially identified due to its NEM sensitivity [25]. NSF acts by dissociating and recycling post-fusion soluble NSF associated protein receptor (SNARE) complexes. Excitingly, the discovery of a mitochondrial localized SNARE, VAMP-1B gives us some reason to expect the existence of an NSF-based membrane fusion system involving mitochondria [26]. It is possible that NSF is acting to regulate futile fission and fusion cycles in mitochondria in role similar to that proposed by Peters et al. [27] in yeast vacuolar dynamic regulation.

In conclusion, we hypothesize that EA/NEM-induced abrogation of mitochondrial fission leads to unchecked mitochondrial fusion. This study also provides the first evidence of a link between MT-based mitochondrial movement and mitochondrial fission. It is also evident that these drugs, because of their rapid, reproducible and specific fusogenic effect in mammalian cultured cells will prove to be valuable tools for the understanding of the mitochondrial fission/fusion dynamic and its effect on other cellular processes.

Acknowledgment

This work was supported by a research grant from the Canadian Institute of Health Research.

Appendix A. Supplementary data

Live mito-eGFP B-SC-1 cell undergoing NEM-induced mitochondrial fusion. Movie data for the cell shown in Fig. 1. NEM was added 30 min after the start of image acquisition. Images were taken every 10 s. Fast mitochondrial movement events are easily visible from the start of acquisition and ending at ~25 min after NEM. Mitochondrial extensions become apparent ~20 min after NEM. Mitochondrial fusion starts to become prevalent at ~20–25 min after NEM addition. Supplementary data associated with this article can be found, in the online version, at doi:10.1016/j.bbrc.2008.08.120.

References

[1] D.A. Rube, A.M. van der Bliek, Mitochondrial morphology is dynamic and varied, Mol. Cell. Biochem. 256-257 (2004) 331–339.
[2] H.M. Heath-Engel, G.C. Shore, Mitochondrial membrane dynamics cristae remodelling and apoptosis, Biochim. Biophys. Acta 1763 (2006) 549–560.
[3] D.C. Chan, Mitochondrial fusion and fission in mammals, Annu. Rev. Cell. Dev. Biol. 22 (2006) 79–99.
[4] V. Anesti, L. Scorrano, The relationship between mitochondrial shape and function and the cytoskeleton, Biochim. Biophys. Acta 1757 (2006) 692–699.
[5] J. Bereiter-Hahn, M. Voth, Dynamics of mitochondria in living cells: shape changes, dislocations, fusion, and fission of mitochondria, Microsc. Res. Tech. 27 (1994) 198–219.
[6] M. Karbowski, R.J. Youle, Dynamics of mitochondrial morphology in healthy cells and during apoptosis, Cell. Death Differ. 10 (2003) 870–880.
[7] K.G. Hales, M.T. Fuller, Developmentally regulated mitochondrial fusion mediated by a conserved, novel, predicted GTPase, Cell 90 (1997) 121–129.
[8] J. Nunnari, W.F. Marshall, A. Straight, A. Murray, J.W. Sedat, P. Walter, Mitochondrial transmission during mating in *Saccharomyces cerevisiae* is determined by mitochondrial fusion and fission and the intramitochondrial segregation of mitochondrial DNA, Mol. Biol. Cell 8 (1997) 1233–1242.
[9] G. Szabadkai, A.M. Simoni, M. Chami, M.R. Wieckowski, R.J. Youle, R. Rizzuto, Drp-1-dependent division of the mitochondrial network blocks intraorganellar Ca^{2+} waves and protects against Ca^{2+}-mediated apoptosis, Mol. Cell 16 (2004) 59–68.
[10] H.M. McBride, M. Neuspiel, S. Wasiak, Mitochondria: more than just a powerhouse, Curr. Biol. 16 (2006) R551–R560.
[11] Y.J. Lee, S.Y. Jeong, M. Karbowski, C.L. Smith, R.J. Youle, Roles of the mammalian mitochondrial fission and fusion mediators Fis1, Drp1, and Opa1 in apoptosis, Mol. Biol. Cell 15 (2004) 5001–5011.
[12] H. Chen, S.A. Detmer, A.J. Ewald, E.E. Griffin, S.E. Fraser, D.C. Chan, Mitofusions Mfn1 and Mfn2 coordinately regulate mitochondrial fusion and are essential for embryonic development, J. Cell Biol. 160 (2003) 189–200.
[13] R.H. Baloh, R.E. Schmidt, A. Pestronk, J. Milbrandt, Altered axonal mitochondrial transport in the pathogenesis of Charcot-Marie-Tooth disease from mitofusin 2 mutations, J. Neurosci. 27 (2007) 422–430.
[14] C. Alexander, M. Votruba, U.E. Pesch, D.L. Thiselton, S. Mayer, A. Moore, et al., OPA1, encoding a dynamin-related GTPase, is mutated in autosomal dominant optic atrophy linked to chromosome 3q28, Nat. Genet. 26 (2000) 211–215.
[15] E. Smirnova, L. Griparic, D.L. Shurland, A.M. van der Bliek, Dynamin-related protein Drp1 is required for mitochondrial division in mammalian cells, Mol. Biol. Cell 12 (2001) 2245–2256.
[16] A. Santel, M.T. Fuller, Control of mitochondrial morphology by a human mitofusion, J. Cell Sci. 114 (2001) 867–874.
[17] K.J. De Vos, V.J. Allan, A.J. Grierson, M.P. Sheetz, Mitochondrial function and actin regulate dynamin-related protein 1-dependent mitochondrial fission, Curr. Biol. 15 (2005) 678–683.
[18] B.J. Soltys, R.S. Gupta, Changes in mitochondrial shape and distribution induced by ethacrynic acid and the transient formation of a mitochondrial reticulum, J. Cell Physiol. 159 (1994) 281–294.
[19] T.J. Bowes, R.S. Gupta, Induction of mitochondrial fusion by cysteine-alkylators ethacrynic acid and *N*-ethylmaleimide, J. Cell Physiol. 202 (2005) 796–804.
[20] B. Singh, R.S. Gupta, Mitochondrial import of human and yeast fumarase in live mammalian cells: retrograde translocation of the yeast enzyme is mainly caused by its poor targeting sequence, Biochem. Biophys. Res. Commun. 346 (2006) 911–918.

[21] B.J. Soltys, R.S. Gupta, Immunoelectron microscopic localization of the 60-kDa heat shock chaperonin protein (Hsp60) in mammalian cells, Exp. Cell Res. 222 (1996) 16–27.
[22] D. Margineantu, R.A. Capaldi, A.H. Marcus, Dynamics of the mitochondrial reticulum in live cells using Fourier imaging correlation spectroscopy and digital video microscopy, Biophys. J. 79 (2000) 1833–1849.
[23] M.K. Knowles, M.G. Guenza, R.A. Capaldi, A.H. Marcus, Cytoskeletal-assisted dynamics of the mitochondrial reticulum in living cells, Proc. Natl. Acad. Sci. USA 99 (2002) 14772–14777.
[24] P.J. Hollenbeck, W.M. Saxton, The axonal transport of mitochondria, J. Cell Sci. 118 (2005) 5411–5419.
[25] V. Malhotra, L. Orci, B.S. Glick, M.R. Block, J.E. Rothman, Role of an *N*-ethylmaleimide-sensitive transport component in promoting fusion of transport vesicles with cisternae of the Golgi stack, Cell 54 (1988) 221–227.
[26] S. Isenmann, Y. Khew-Goodall, J. Gamble, M. Vadas, B.W. Wattenberg, A splice-isoform of vesicle-associated membrane protein-1 (VAMP-1) contains a mitochondrial targeting signal, Mol. Biol. Cell 9 (1998) 1649–1660.
[27] C. Peters, T.L. Baars, S. Bubler, A. Mayer, Mutual control of membrane fission and fusion proteins, Cell 119 (2004) 667–678.